Acylpeptide hydrolase is a component of the cellular response to DNA damage

Article (Accepted Version)

Acylpeptide Hydrolase is a Component of the Cellular Response to DNA Damage

Zhihong Zeng[1], Stuart L. Rulten[1], Claire Breslin, Anastasia Zlatanou[2], Victoria Coulthard, and Keith W. Caldecott*

Genome Damage and Stability Centre, University of Sussex, Falmer, Brighton

Corresponding author; Tel, 44 1273 877519; k.w.caldecott@sussex.ac.uk
[1]These authors contributed equally
[2]Current address; Dept. Pathology and Laboratory Medicine, University of North Carolina, Chapel Hill, US
Running Title; Acylpeptide hydrolase and the DNA damage response

Abstract

Acylpeptide hydrolase (APEH) deacetylates N-alpha-acetylated peptides and selectively degrades oxidised proteins, but the biochemical pathways that are regulated by this protease are unknown. Here, we identify APEH as a component of the cellular response to DNA damage. Although APEH is primarily localised in the cytoplasm, we show that a sub-fraction of this enzyme is sequestered at sites of nuclear damage following UVA irradiation or following oxidative stress. We show that localization of APEH at sites of nuclear damage is mediated by direct interaction with XRCC1, a scaffold protein that accelerates the repair of DNA single-strand breaks. We show that APEH interacts with the amino-terminal domain of XRCC1, and that APEH facilitates both single-strand break repair and cell survival following exposure to H_2O_2 in human cells. These data identify APEH as a novel proteolytic component of the DNA damage response.

1. Introduction

Alpha acetylation of the amino-terminal amino acid of proteins (Nα-acetylation) is a common protein post-translational modification in eukaryotes, occurring on 50-90% of proteins [1,2]. Although the precise role of this modification is unclear, it is evolutionarily conserved and is required for a broad range of protein functions and cellular processes. For example, in budding yeast, Nα-acetylation of Orc1 and Sir3 is required to maintain gene silencing, demonstrating an important role for Nα-acetylation in regulating chromatin structure [3,4]. In the case of Sir3, Nα-acetylation is required for binding unmethylated H3K79 and thus targeting of Sir3 to appropriate genomic sites in order to establish heterochromatin [5,6]. In addition, in human cells, Bcl-xL controls the level of Nα-acetylation of key apoptotic mediator proteins and thereby regulates apoptosis [7].

In contrast to the acetylation of amino acid side chains, Nα-acetylation of peptide amino termini is not reversible. However, cellular levels of Nα-acetylation are regulated by a cytosolic serine protease denoted acylpeptide hydrolase (APEH), which can remove the Nα-acetylated amino-terminal amino acid from oligopeptides [8] and decreases the extent of Nα-acetylation in many proteins [9]. Intriguingly, APEH also

possesses endo and/or exopeptidase activity on oxidised or glycated proteins and so is also denoted oxidised protein hydrolase [10,11]. It is currently unclear whether the endo/exopeptidase activity of APEH is dependent on its acylpeptide hydrolase activity but, in support of this idea, the loss of Nα-acetylation destabilises and/or promotes proteolysis of some proteins [12,13]. Recently, APEH was also reported to regulate the activity of the proteosome [14].

Loss or inhibition of APEH activity is implicated in elevated T cell proliferation and small cell lung cancer [9,15]. However, the biochemical pathways that are regulated by APEH are unknown. Here, we show that APEH is a component of the cellular response to chromosomal DNA damage, following oxidative stress. We show that APEH interacts directly with the DNA single-strand break repair (SSBR) scaffold protein XRCC1 and that this interaction mediates recruitment of APEH both into the nucleus and at sites of nuclear damage. Moreover, we show that in human cells APEH promotes both the repair of chromosomal single-strand breaks (SSBs) and cellular resistance to oxidative stress. These data identify APEH as a novel component of the DNA damage response, and we suggest that this protease facilitates protein metabolism at chromosomal sites of DNA strand breakage.

2. Materials and Methods

2.1. Direct fluorescence microscopy.

$1x10^5$ A549 or EM9 cells were seeded on glass cover-slips and after 48-hr transfected (Genejuice; Merck) with 1μg peGFP-APEH and 1μg either of pmRFP-C1, pmRFP-XRCC1, or pmRFP-$XRCC1^{F67A}$. 24-hr after transfection, cells were washed in PBS and treated with 10mM H_2O_2 (in PBS) for 10min on ice and then incubated in drug-free medium at 37°C for the times indicated. Cells were then fixed in PBS containing 4% paraformaldehyde for 2-5 min, permeabilized in 0.2% Triton X-100 for 2 min, rinsed in PBS, and counterstained with 0.000025% DAPI (4',6'-diamidino-2-phenylindole) for 5 min. Coverslips were mounted in Vectashield (Vector Labs) and analyzed with a Zeiss Axioplan 2 fluorescence microscope. Photographs were taken at a magnification of x100 with appropriate filters and where indicated cells scored for sub-cellular localisation of GFP-APEH and mRFP-XRCC1.

2.2. Laser microirradiation.

Human A549 cells were seeded onto glass-bottom dishes (Mattek) and co-transfected with peGFP-APEH and pRFP-XRCC1 [16] as described above. 24-hr after transfection, cells were incubated for 30 min with 10 μg/ml Hoechst 33258 at 37°C. Selected cells were then irradiated with a 351-nm UVA laser focused through a 40X/1.2-W objective using a Zeiss Axiovert equipped with LSM 520 Meta. UVA (10.47 μJ) was introduced to an area of approximately 15μm x 2μm (approximately 0.35 μJ/μm^2).

2.3. Subcellular fractionation.

2x10^7 A549 cells were harvested by trypsinisation and resuspended in 1ml fractionation buffer (15mM Tris-pH7.5, 0.3M sucrose, 15mM NaCl, 5mM $MgCl_2$, 0.1mM EGTA, 0.5mM DTT, 0.1mM PMSF). An equal volume of fractionation buffer + 0.4% IGEPAL was added and the suspension was mixed and incubated on ice for 10 min. The lysate was then layered onto 5ml extraction buffer containing 1.2M sucrose and spun at 10,000g for 20min at 4°C. The top layer containing the cytoplasm was removed and the nuclear pellet washed and resuspended in 500μl immunoprecipitation buffer (20mM Tris-HCl pH7.5, 10mM EDTA, 100mM NaCl, 1% Triton X-100, 1% Sigma protease inhibitor cocktail).

2.4. DNA constructs.

pACT-23 is a human cDNA library clone encoding OPH/APEH (from now on denoted APEH) recovered using XRCC1 as bait (data not shown). To construct pcD2E-FLAG-APEH, encoding FLAG-tagged APEH, the APEH ORF was amplified from pACT-23 using forward [5'- gcgaattcagaggagactatg*gactacaaagatgacgatgacaa*ggaacgtcagg-3'] and reverse [5'-
gcgaattctcagctgcccaagtgtgtgc-3'] primers containing *Eco*RI restriction sites (underlined) and the FLAG ORF (italicised and underlined) and subcloned into pTOPO2.1 (Invitrogen) as described by the manufacturer. The *Eco*RI fragment harbouring the FLAG-APEH ORF was then subcloned into the *Eco*RI site of

pcD2E[17,18]. To create peGFP-APEH, the APEH ORF was amplified from pact 23 using forward [5'-cgaattctgatggaacgtcaggtgctg-3'] and reverse [5'-gcggatccgtcagctgcccaagtgtgtgc-3'] primers containing *Eco*RI and *Bam*HI restriction sites (underlined) and cloned into the *Eco*RI/*Bam*HI sites in peGFP-C3 (Clontech). To create pSUPER-APEH, 64mer forward [5'-gatcccc*GGACAAATCGCCCATCAGA*ttcaagaga*TCTGATGGGCGATTTGTCC*tttttggaa-3'] and reverse [5'agcttttccaaaaa*GGACAAATCGCCCATCAGA*tctcttgaa*TCTGATGGGCGATTTGTCC*ggg-3'] oligonucleotides (targeted APEH sequence in italics) were annealed and ligated into the *Bgl*II and *Hind*III sites of pSUPER (Oligoengine)[19]. To create pcD2E-FLAG-APEH^{TR}, encoding shRNA targeting resistant FLAG-tagged APEH, pcD2E-FLAG-APEH was mutated using a Quickchange XL site-directed mutagenesis kit (Stratagene) and appropriate forward [5'-gatgctggacaaatcgccGatTCgCtacatccctcaggtg-3'] and reverse [5'-cacctgagggatgtaGcGAatCggcgatttgtccagcatc-3'] primers and confirmed by sequencing (non-coding sequence changes are in capitals). To create pFastBac-APEH, the APEH ORF was amplified by PCR from pACT-23 using appropriate forward [5'-aaaaggatccatggaacgtcaggtgctgctg-3'] (*Bam*HI site underlined) and reverse primers and cloned into pTOPO2.1. A *Bam*HI/*Not*I fragment encompassing the APEH ORF cloned into the *Bam*H1/*No*tI sites of pFastBac-HT-B (Invitrogen). The yeast 2-hybrid constructs pAS-*XRCC1* [20], pAS-*Lamin* [21], pACT-*Pol*β [22], pACT-*PNKP*[22], pAS-*XRCC1*$^{75-212}$ [23], pAS-*XRCC1*$^{1-159}$ [23] have been described previously. The yeast 2-hybrid constructs pGBKT7-*XRCC1*^{F67A}, pGBKT7-*XRCC1*$^{242-533}$, and pASLig3α were constructed by standard protocols and pAS-Lamin and pAS-p53 were kind gifts from Luke Alphey.

2.5. Recombinant human APEH protein and anti-APEH antibody.

Recombinant human histidine tagged APEH (His-APEH) was generated in Sf9 cells using pFastBac-APEH and the Bac-to-Bac baculovirus expression system (Invitrogen). Recombinant human His-APEH protein was purified from infected Sf9 by immobilized metal chelate chromatography using Ni-NTA agarose (Qiagen) and used as antigen to raise rabbit anti-APEH polyclonal antibody SY0999 (Eurogentec). SY0999 was affinity purified against recombinant human APEH prior to use.

2.6. APEH depletion by RNA interference.

For transient APEH depletion, A549 cells were transfected (METAFECTENE PRO, Biontex) with a SMARTpool (Thermo Scientific Dharmacon) comprised of the double-stranded siRNA oligoribonucleotides 5-GCAUGGAGAACAUUCGAUU-3', 5'-CAAAAGCACCCACGCAUUA-3', 5'-GGACAAAUCGCCCAUCAGA-3' and 5'-GAGGCUGGCUUUCCUUUCA-3'. For stable APEH depletion, the most effective of the four SMARTpool siRNAs was identified and the corresponding oligodeoxyribonucleotide sequence (5'-GGACAAATCGCCCATCAGA-3') cloned into the shRNA expression vector pSUPER, creating the shRNA construct pSUPER-APEH (see above). $3x10^7$ A549 cells were then co-transfected with pCI-puro and either empty pSUPER or pSUPER APEH and single transfected clones selected for 6-10 days in medium containing 0.8μg/ml puromycin and analysed by immunoblotting for levels of APEH depletion. For complementation analysis, a A549 APEH-depleted (clone 3) was transfected with empty pCD2E or pCD2E-$APEH^{TR}$ and selected in the presence of 1.5mg/ml G418 and 0.8μg/ml Puromycin for 2-3 weeks. Drug-resistant clones were pooled, expanded, and examined by immunoblotting for normal or near-normal levels of APEH protein.

2.7. Immunoprecipitation.

Total cell extract (100μg total protein) or nuclear extract (0.6 mg nuclear protein) from the indicated A549 cells was pre-cleared for 2h at 4°C with 60 μl protein G-Sepharose beads (Sigma) and the pre-cleared extract then incubated with 5μl of rabbit anti-human APEH polyclonal antibody (SY0999) or rabbit IgG (DAKO) on a carousel at 4°C overnight in a final volume of 300μl immunoprecipitation (IP) buffer [20 mM Tris-HCl, pH 7.5, 10 mM EDTA, 100 mM NaCl, 1% Triton X-100, 10% Glycerol, and 1x protease inhibitor cocktail (Sigma)], followed by 30 μl protein G-Sepharose beads for 1 h at 4°C with gentle agitation. Beads were then pelleted in a microfuge, washed with IP buffer (3x300μl), and bound proteins eluted by heating in 55 μl of 2x SDS-PAGE sample buffer at 90°C for 5 min. Clarified protein samples were fractionated by SDS-PAGE, transferred to nitrocellulose, and immunoblotted with the anti-phospho-XRCC1 rabbit polyclonal antibody A300-059A (Bethyl) and the anti-APEH rabbit polyclonal

antibody, SY0999.

2.8. Yeast two-hybrid analysis.

Pooled populations of Yeast Y190 transformants harbouring the indicated pGBKT7/pAS and pACT fusion protein constructs were plated onto minimal media lacking Leu and Trp to select for both plasmids or on media additionally lacking histidine and containing 25mM 3-aminotriazole (3-AT) to select for activation of the *His3* reporter gene. In addition, colonies from Leu-, Trp- control plates were examined for β-galactosidase (β-gal) activity by filter lift assays, to detect activation of the β-*gal* reporter gene. Equivalent expression levels of pAS DNA binding domain or pACT activation domain fusion proteins were confirmed by immunoblotting using the anti-APEH rabbit polyclonal antibody SY0999 and the anti-XRCC1 rabbit polyclonal antibody A300-059A (Bethyl).

2.9. Clonogenic survival assays.

The indicated A549 cells were plated (500/plate) in 10-cm dishes in duplicate and incubated for 4 h at 37°C. Cells were rinsed with PBS (x2) and either mock treated or treated with the indicated concentration of either H_2O_2 in PBS for 15 min at room temperature or with methyl methanesulphonate (MMS) or camptothecin (CPT) in complete medium for 1 hr at 37°C. After treatment, cells were rinsed with PBS (x2) and incubated for 10-14 days in drug-free medium at 37°C to allow formation of macroscopic colonies. Colonies were fixed in ethanol (95%), stained with 1% methylene blue/70% ethanol and colonies of >50 cells were counted. Survival was calculated and expressed graphically using the equation 100 X [mean colony number (treated plates)/mean colony number (untreated plates)].

2.10 Alkaline single-cell agarose-gel electrophoresis (alkaline comet assay).

Sub-confluent monolayers of the indicated A549 cells were trypsinized and diluted to $4x10^5$ cells/ml immediately prior to mock treatment or treatment with 0.1mM H_2O_2 in PBS for 20 min on ice. Cells were then washed in ice-cold PBS and incubated in fresh drug-free medium at 37°C for the indicated repair period. Cells were then collected and

subjected to single-cell agarose gel electrophoresis. In brief, cell suspensions were quickly mixed with 200µl low melting point agarose type VII (Sigma Aldrich) and 150ul spread onto 0.6% mini agarose gels on frosted slides on ice. Slides were maintained at 4°C for 30 minutes to set and then immersed in ice-cold lysis buffer (2.5M NaCl, 100mM EDTA, 1% Triton X-100 pH 10) for 1 hr in the dark. After rinsing in ice-cold dH2O (x3), slides were incubated in alkaline electrophoresis buffer (50 mM NaCl, 1mM EDTA and 1% DMSO) for 45 min to allow DNA unwinding and then subject to electrophoresis for 25 minutes at 12V. Slides were then immersed in neutralisation buffer (0.4 M Tris PH 7.0) for at least 3 min at room temperature. Nuclei acid was stained with SYBR green (1:10000 dilution, Sigma) and visualised by fluorescence microscopy (Nikon Eclipse E400) at 20X magnification. The average comet tail moment for 100 cells per sample was determined using Comet Assay III software (Perceptive Instruments) and the mean of this value (+/- s.e.m) for at least three independent experiments per sample was calculated. Note that the comet tail moment is the product of the tail length and the fraction of DNA in the tail.

3. Results

3.1. APEH interacts with XRCC1 in yeast 2-hybrid assays

A previous yeast 2-hybrid (Y2H) screen of a human cDNA library for proteins that interact with the DNA strand break repair protein XRCC1 identified PNKP [24], APTX [21], Pol β [20], and DNA ligase IIIα [24] as protein partners. In this same screen, we also recovered cDNAs encoding the protein acylpeptide hydrolase (APEH)(Fig.1A). Both *His3* and *βgal* reporter genes indicative of protein-protein interaction were activated in yeast Y190 cells harbouring pACT-*APEH* and pAS-*XRCC1*, whereas neither reporter gene was activated in cells harbouring pACT-*APEH* and either of the unrelated control constructs, pAS-*Lig3α*, pAS-*p53*, or pAS-*Lamin* (Fig.1A). Similar results were observed with the opposite vector configuration; with XRCC1 and APEH expressed as fusion proteins with the GAL4 activation and DNA binding domains, respectively (Supplementary Fig.1).

To confirm the interaction between XRCC1 and APEH biochemically we examined whether recombinant human XRCC1 and APEH would co-

immunoprecipitate from cell extract from Y190 yeast cells harbouring pAS-*XRCC1* and pACT-*APEH*. Indeed, anti-XRCC1 antibody precipitated both recombinant XRCC1 and APEH from this protein extract, whereas control IgG did not (Fig.1B, compare lanes 2 & 3). In contrast, anti-XRCC1 antibodies failed to immunoprecipitate APEH from yeast cell extract lacking recombinant XRCC1, ruling out that the recovery of APEH by anti-XRCC1 antibodies was due to non-specific cross-reactivity of the antibody (Fig.1B, compare lanes 4 & 5).

Finally, additional Y2H analyses employing a variety of truncated or mutated derivatives of XRCC1 revealed that APEH interacts with the amino-terminal domain (NTD) of XRCC1 (Fig.1C), which is the same region of XRCC1 that interacts with DNA polymerase β [25]. Indeed, a single point mutation (F67A) within the XRCC1 NTD that disrupts interaction with Pol β [26,27] similarly disrupted interaction with APEH, confirming that the interaction site in XRCC1 for Pol β and APEH overlap (Fig.1C). The lack of interaction between APEH and XRCC1 fragments lacking an intact NTD did not reflect instability of the mutant proteins, because these proteins retained the ability to interact with PNKP, which binds XRCC1 downstream of the NTD (Fig.1C). Together, these data identify APEH as an XRCC1-interacting protein.

3.2 APEH is a component of the cellular response to oxidative stress and is physically associated with XRCC1 in mammalian cells.

To examine whether APEH might be a component of the cellular response to oxidative stress, we compared the sub-cellular localisation of the GFP-tagged human protein before and after treatment of transiently-transfected A549 cells with H_2O_2. Consistent with previous observations [28], ~60% of transiently-transfected cells exhibited cytosolic GFP-APEH signal and ~40% exhibited pan-cellular GFP-APEH (Fig.2A). However, the fraction of cells with pan-cellular GFP-APEH increased to ~75% following treatment with H_2O_2, suggesting that nuclear import and/or retention of GFP-APEH increased following oxidative stress (Fig.2A). Similar to mRFP-XRCC1, GFP-APEH accumulated rapidly at sites of nuclear damage following irradiation with a UVA laser (Fig.2B). Together, these data suggest that APEH is a component of the cellular response to nuclear damage induced by UVA or H_2O_2-induced oxidative stress.

We next examined whether APEH is physically associated with XRCC1 in human A549 cells. Notably, anti-APEH antibodies co-immunoprecitated XRCC1 from

whole cell extract prepared from human A549 cells, whereas control IgG did not (Fig.3A). However, because our immunofluorescence experiments suggested that APEH and XRCC1 are primarily located in different cellular compartments we repeated these experiments using protein extract prepared from highly purified nuclei, to rule out that this interaction was an artifact of mixing the subcellular compartments during cell lysis. Subcellular fractionation confirmed that APEH and XRCC1 are primarily located in different cellular compartments (Fig.3B). Indeed, we failed to detect any APEH in nuclear extracts with the antibodies available to us, either before or after H_2O_2 treatment, suggesting that very little if any APEH is present in nuclei. Nevertheless, anti-APEH antibodies immunoprecipitated XRCC1 from nuclear extracts both before and after H_2O_2 treatment (~1% and ~3% of total nuclear XRCC1, respectively; Fig.3C). Despite this, we still could not detect APEH in the nuclear immunoprecipitate (data not shown). Consequently, to confirm that co-immunoprecipitation of APEH and XRCC1 reflected physical association of these proteins, rather than nonspecific binding of XRCC1 by anti-APEH antibody, we employed nuclear extract from A549 cells in which APEH was stably depleted by ~90% by shRNA (Fig.3D, *top*). Importantly, whereas, anti-APEH antibodies again immunoprecipitated XRCC1 from wild-type A549 cell extract, they failed to do so from APEH-depleted cell extract, confirming that a small amount of cellular XRCC1 and APEH are physically associated (Fig.3D, *bottom*).

3.3. XRCC1 promotes APEH nuclear localisation and recruitment at sites of H_2O_2-induced nuclear damage.

XRCC1 interacts with multiple proteins during SSBR including PARP1, Lig3α, PNKP, APTX, APLF, and DNA polymerase-β [29]. These interactions serve a variety of functions including enzymatic stimulation, stabilisation, and recruitment of the XRCC1 partners at sites of DNA damage. We thus examined whether interaction with XRCC1 might be important for the nuclear localisation of APEH, since this protein lacks an identifiable nuclear localisation signal. Indeed, the majority of GFP-APEH expressed in XRCC1-mutant (EM9) CHO cells localised to the cytoplasm, but co-expression of mRFP-XRCC1 resulted in redistribution of this protease to the nucleus, as indicated by an increase in the fraction of cells with pan-cellular GFP-APEH (Fig.4A). In contrast, co-expression of GFP-APEH with either mRFP or mRFP-XRCC1^{F67A}, which cannot

bind the protease, failed to promote nuclear localisation (Fig.4A). We noticed that H_2O_2-treatement increased the level of nuclear GFP-APEH only by a small extent in these experiments, presumably because the high level of mRFP-XRCC1 expression promoted APEH nuclear localisation even in the absence of H_2O_2. However, GFP-APEH did co-localise with mRFP-XRCC1 in sub-nuclear foci following H_2O_2-treatment, confirming that GFP-APEH accumulated with XRCC1 at sites of DNA strand breakage (Fig.4B, *middle panels*). Moreover, GFP-APEH failed to accumulate into nuclear foci in EM9 cells following H_2O_2-treatment in the absence of mRFP-XRCC1 co-expression (Fig.4B, *top panels*), or if co-expressed with mRFP-XRCC1^{F67A} that cannot bind APEH (Fig.4B, *bottom panels*). We conclude from these experiments that the XRCC1 interaction promotes the nuclear localization of GFP-APEH and the recruitment of this protease to sites of DNA strand breakage after H_2O_2 treatment.

3.4. APEH promotes chromosomal SSBR following H_2O_2 treatment.

Given that APEH is recruited to sites of DNA damage by interaction with XRCC1, we examined whether the protease influences the rate of repair of oxidative chromosomal DNA strand breaks. Indeed, APEH siRNA significantly reduced the rate at which oxidative DNA strand breaks declined in H_2O_2 treated A549 cells (Fig.5B, *top*). Whilst the defect in SSBR in APEH-depleted cells was quite small it was statistically significant. Moreover, it is consistent with defects in core SSBR proteins such as XRCC1 and PNKP, which also only slow the rate of SSBR, by up to ~5-fold [22,30]. Similar results were observed in A549 cells that were stably depleted of APEH by expression of anti-APEH shRNA, and expression of shRNA-resistant APEH mRNA restored both the level of APEH protein and the rate of DNA strand break repair to normal (Fig.5B, *bottom*). Together, these data suggest that APEH promotes the rate of repair of DNA strand breaks induced by DNA oxidation.

3.5. APEH promotes cellular resistance to H_2O_2

Finally, we examined whether APEH depletion resulted in hypersensitivity to oxidative stress, in clonogenic survival assays. Indeed, treatment of human A549 cells with a pool of three anti-APEH siRNA molecules (Fig.6A), or stable expression of APEH shRNA (Fig.6B), significantly increased sensitivity to H_2O_2-induced oxidative damage. In

contrast, APEH-depleted cells were not hypersensitive to either methyl methanosulphonate (MMS) or camptothecin (CPT), genotoxic agents that kill cells by mechanisms independent of oxidative stress (Fig.6C & 6D). Moreover, expression of shRNA-resistant APEH mRNA restored normal levels of survival in APEH-depleted A549 cells following H_2O_2 treatment, confirming that APEH promotes cellular resistance to oxidative stress (Fig.6B). Together, these data demonstrate that APEH promotes both the rate of chromosomal DNA strand break repair and cell survival in human cells, following H_2O_2 treatment.

Discussion

Acylpeptide hydrolase (APEH) is a cytosolic serine protease that removes Nα-acetylated amino acids from the amino terminus of peptides and degrades oxidised proteins [8,10,11]. Overexpression of APEH/OPH in COS-7 cells reduces the accumulation of oxidised proteins during treatment with H_2O_2 or paraquat, and APEH deletion is implicated in renal carcinoma and small cell lung carcinoma [15,31,32]. In addition, inhibition of APEH promotes T cell proliferation [9]. Despite the biological importance of APEH, however, the biochemical pathways influenced by this protease are unknown.

Here, we report that APEH is a novel component of the mammalian DNA damage response. We found using yeast 2-hybrid analyses that APEH interacts directly with the DNA single-strand break repair (SSBR) scaffold protein, XRCC1. The interaction with APEH is mediated via the amino terminal domain (NTD) of XRCC1, a region that also binds DNA polymerase β, suggesting that these two interactions are likely to be mutually exclusive. A similar situation is observed for the interactions between XRCC1 and PNKP, APLF, and APTX, all of which interact with XRCC1 via a centrally located cluster of CK2 phosphorylation sites [16,21,22,33,34]. Intriguingly, co-immunoprecipitation experiments revealed that only a small sub-fraction of endogenous APEH is bound to XRCC1, and that this sub-fraction increases approximately ~3-fold following treatment with H_2O_2. Consistent with this observation, although GFP-tagged APEH was located primarily in the cytoplasm of transfected cells, a sub-fraction of GFP-APEH was recruited into nuclei following treatment with H_2O_2, as suggested by the fraction cells that displayed pan-cellular GFP-

APEH fluorescence. Over-expression of wild type human RFP-XRCC1 also increased the fraction of cells displaying pan-cellular GFP-APEH, even in the absence of H_2O_2 treatment, and this was prevented by the F67A mutation that disrupts interaction with APEH. We do not yet know if the H_2O_2-mediated increase in pan-cellular GFP-APEH is also mediated by interaction with XRCC1, but this seems likely. Similarly, we do not know why H_2O_2 treatment and/or XRCC1 over-expression increased the fraction of cells with pan-cellular APEH, rather than increasing the level of nuclear GFP-APEH in all cells. One possibility is that other factors also influence the sub-cellular localisation of APEH, such as cell cycle position and/or sub-cellular localization of other binding partners. Finally, we noted that treatment with leptomycin B also promoted an increase in the fraction of A549 cells with pan-cellular GFP-APEH (unpublished observations), suggesting that the cytoplasmic localisation of GFP-APEH is promoted by nuclear export.

Importantly, a sub-fraction of GFP-APEH accumulated at sites of nuclear damage induced by either UVA laser or H_2O_2. In the latter case, we demonstrated that this event was XRCC1 dependent, since GFP-APEH relocalised into H_2O_2-induced nuclear foci when co-expressed with wild type RFP-XRCC1 but not with RFP-XRCC1^{F67A}. We employed UVA laser and H_2O_2 in these experiments because of the established role of APEH in degrading oxidised proteins, but we cannot rule out that APEH plays a more general role at other types of DNA strand breakage. Consistent with these data, depletion of APEH in human A549 cells reduced the rate of chromosomal DNA strand-break repair following H_2O_2 treatment. Whilst the impact of APEH depletion on DNA strand break repair was mild it is important to note that the loss of even core components of this process such as PARP1 and XRCC1 slow SSBR only ~5-fold, attesting to the enzymatic resilience and/or redundancy within this pathway [22,30]. Because the majority (>99.5%) of DNA strand breaks induced by DNA oxidation are SSBs [35] it is likely that the reduced rate of DNA strand break repair in APEH depleted cells reflects a reduced rate of SSBR. This conclusion is consistent with the interaction of APEH with XRCC1, since the latter is a key regulator of chromosomal SSBR [29]. In addition to accelerating SSBR, APEH was also required for cellular resistance to oxidative stress, as measured by the hypersensitivity of APEH-depleted cells to H_2O_2 in clonogenic survival assays. This was not an off-target effect of shRNA because stable expression of shRNA-resistant APEH restored normal levels of resistance to H_2O_2. In contrast, we did not observe hypersensitivity to either methyl

methanesulphonate (MMS) or camptothecin (CPT), two genotoxins that induce SSBs independently of oxidative stress.

What role might APEH play at chromosomal SSBs? APEH is important for degrading oxidised membrane and cytoplasmic proteins [10,28,32,36]. However, a recent proteomic analysis identified a broad range of both nuclear and cytoplasmic proteins that exhibited altered levels of Nα-acetylation if APEH activity was inhibited, suggesting that the number and distribution of APEH substrates may be much larger than previously thought [9]. Our finding that a sub-fraction of APEH is sequestered at sites of nuclear DNA damage is consistent with this possibility and raises the possibility that this protease processes one or more protein components of damaged chromatin. One possibility is that APEH modulates chromatin compaction at chromosomal SSBs by controlling the Nα-acetylation status of one or more chromatin regulators, analogous to the role played by Nα-acetylation on Orc1 and Sir3 function in budding yeast [3-6]. Perhaps consistent with this, we have observed that APEH over-expression represses silencing of a telomeric URA3 gene in budding yeast, silencing of which is known to be dependent on Nα-acetylation of Orc1 and Sir3, is consistent with this model (unpublished observations).

An alternative model for APEH function is that the enzyme is required for removal or degradation of oxidised proteins during SSBR. Protein oxidation may be particularly prevalent at sites of SSBs, because the elevated concentration of ADP-ribose arising from poly (ADP-ribose) synthesis at SSBs can lead to protein glycoxidation and oxidation [37-40]. Oxidised chromatin proteins might require removal and degradation not only to allow access for repair, but also to prevent them from perturbing chromatin function and the epigenetic code. A mechanism for degrading oxidised histone proteins that employs the 20S proteosome has been described previously [41,42]. Whilst APEH has been reported to regulate the activity of the proteasome [14], it is possible that APEH provides an alternative mechanism for degrading oxidised histones, since it has also been reported to function independently of the proteosome [28]. It is also possible that the acylpeptide hydrolase and oxidised protein hydrolase activities of APEH function synergistically in this respect, since removal of the Nα-acetylated terminal amino acid from proteins has been reported to promote protein instability and degradation.

In summary, we have identified acylpeptide hydrolase (APEH) as a novel component of the mammalian DNA damage response. We show that APEH is recruited

at sites of DNA strand breakage induced by H_2O_2 by direct interaction with XRCC1, and that APEH promotes both the rapid repair of chromosomal SSBs and cellular resistance to H_2O_2-induced oxidative stress. Based on these data, we speculate that APEH is required during the repair of SSBs to promote the metabolism or turnover of chromatin proteins at sites of DNA breakage.

Acknowledgements

The work was supported by BBSRC (BB/C516595/1) and MRC (G0901606/1) grants to KWC.

Figure legends

Fig.1. XRCC1 Interacts with APEH in Yeast 2-hybrid Assays. [A] Yeast Y190 cells harbouring the indicated GAL4 activation domain (pACT) and DNA binding domain (pAS) expression constructs encoding full-length XRCC1, APEH, DNA ligase IIIα (Lig3α), DNA polymerase β (Polβ), or Lamin, were examined for activation of the 2-hybrid reporter genes *His3* and *LacZ* ('βgal') as described in Experimental Procedures. **[B],** Anti-XRCC1 and control IgG immunoprecipitates recovered from cell extract from Y190 cells harbouring pAS-*XRCC1* and pACT-*APEH* (lanes 2, 3 & 4), or as an additional negative control pAS-*Lig3α* and pACT-*APEH* (lane 5), were immunoblotted for XRCC1 and APEH. **[C]** *Top***,** Yeast Y190 cells harbouring the indicated pACT full-length expression constructs and DNA binding domain (pAS or pGBKT7; "pGB") truncated XRCC1 expression constructs were examined for activation of the 2-hybrid reporter genes *His3* and *LacZ* ('βgal'), as described above. *Bottom,* Cartoon summarizing the truncated/mutated XRCC1 proteins employed to map the site of APEH interaction. Interaction (+) or lack of interaction (-) with APEH as measured by activation of the *His3* and *LacZ* reporter genes is indicated.

Fig.2. Relocalisation of GFP-APEH in response to UVA laser or H_2O_2-induced damage. A549 transiently transfected with peGFP (GFP) or peGFP-APEH (GFP-APEH) were mock-treated or treated with 10mM H_2O_2 on ice for 10 min followed by incubation in drug-free medium at 37°C for 20 min or 1 hr. GFP proteins were

visualised in fixed cells by direct immunofluorescence microscopy and scored for sub-cellular localisation (*Bottom*). *Top*, representative images of cytoplasmic (*left*) and pan-cellular (*right*) GFP-APEH. Note that we failed to detect cells with exclusively nuclear GFP-APEH (blue). **[B]** A549 cells transiently transfected with peGFP-APEH and pmRFP-XRCC1 were irradiated with a UVA laser and visualised by fluorescent microscopy before and 2-min after UVA irradiation. Representative images are presented.

Fig.3. APEH and XRCC1 physically interact. [A], Whole-cell extract from human A549 cells was immunoprecipitated with rabbit IgG or anti-APEH rabbit polyclonal antibody and aliquots of the input (2%; 'In'), unbound column flow-through (3%;'U'), final column wash (3%; 'W'), and immunoprecipitate (67%; 'P') were fractionated by SDS-PAGE and immunoblotted for APEH (top) and XRCC1 (bottom). **[B]** *Top*; Aliquots (~15μg total protein) of whole-cell, cytoplasmic, and nuclear extract from A549 cells was fractionated by SDS-PAGE and immunoblotted for APEH, XRCC1, and α-tubulin. **[C]** Nuclear extract from mock-treated (*top*) or H_2O_2-treated (*bottom*) A549 cells was immunoprecipitated with rabbit IgG or anti-APEH rabbit polyclonal antibody and aliquots of the input (2%; 'In'), unbound material (2%; 'U'), final column wash (3%; 'W'), and immunoprecipitate (67%; 'P') were fractionated by SDS-PAGE and immunoblotted for XRCC1. **[D]** *Top*, Aliquots of whole cell extract from wild type and APEH-depleted A549 cells were fractionated by SDS-PAGE and immunoblotted for APEH and actin. *Bottom*, nuclear extract from H_2O_2-treated wild type or APEH-depleted A549 cells was immunoprecipitated with anti-APEH rabbit polyclonal antibody and aliquots of the indicated samples fractionated and immunoblotted for XRCC1 as described above.

Fig.4. XRCC1 promotes APEH nuclear localisation and recruitment at sites of H_2O_2-induced nuclear damage. [A] Sub-cellular localisation of GFP-APEH in *XRCC1*-mutant EM9 CHO cells co-transfected with mRFP ('RFP'), mRFP-XRCC1 ('RFP-XRCC1'), or mRFP-XRCC1^{F67A} ('RFP-F67A') in the absence of H_2O_2 treatment ('Unt') or 20 min or 60 min following H_2O_2 treatment. **[B]** Sub-nuclear localisation of GFP-APEH in *XRCC1*-mutant EM9 CHO cells co-expressing mRFP-XRCC1 or mRFP-XRCC1^{F67A} in the absence of H_2O_2 treatment and 20 min after H_2O_2 treatment. Representative images are shown.

Fig.5. APEH promotes chromosomal SSBR following oxidative stress. [A] DNA strand breaks measured in mock-transfected A549 cells ('A549') and A549 cells transiently transfected with APEH siRNA ('KD') prior to ('untreated') or at the indicated times after treatment with 0.1mM H_2O_2. DNA strand breaks were quantified as the mean comet tail moment of 100 cells per data point and are the average (+/- SEM) of five independent experiments. Data for A549 versus KD were compared by two-way ANOVA with replication (*p=0.008*). Significant data points (identified by Bonferroni multiple comparisons tests) are indicated by asterisks. **[C]** DNA strand breaks measured as above in A549 cells, A549 cells stably transfected with APEH shRNA construct ('KD'), and A549 cells stably-transfected with APEH shRNA construct and either empty vector ('KD+V') or expression construct encoding shRNA-resistant APEH ('KD+APEH'). Data are mean (±SEM) of four independent experiments and data sets were compared pair wise by two-way ANOVA with replication. Significantly different data sets were KD versus KD+APEH, *p=0.03* and KD-V versus KD+APEH, *p=0.047*. Significant data points (identified by Bonferroni multiple comparisons tests) are indicated by asterisks.

Fig.6. APEH promotes cellular resistance to oxidative stress. [A] Clonogenic survival following H_2O_2 treatment in mock-transfected A549 cells ('Control') and A549 cells transiently transfected with APEH siRNA. Data are the mean (+/- SEM) of at least three independent experiments. **[B]** Clonogenic survival following H_2O_2 treatment in A549 cells, A549 cells stably transfected with APEH shRNA construct ('KD'), and A549 cells stably-transfected with APEH shRNA construct and either empty vector ('KD+V') or expression construct encoding shRNA-resistant APEH ('KD +APEH'). Data as above. **[C]** Clonogenic survival following treatment with methyl methanesulphonate (MMS) in A549 cells ('control') and A549 cells stably transfected with APEH shRNA construct ('KD'). Data as above. **[D]** Clonogenic survival following treatment with camptothecin (CPT) in A549 cells ('control') and A549 cells stably transfected with APEH shRNA construct ('KD'). Data as above.

[1] J.L. Brown, W.K. Roberts, Evidence that approximately eighty per cent of the soluble proteins from Ehrlich ascites cells are Nalpha-acetylated, J Biol Chem. 251 (1976) 1009–1014.

[2] X. Zhang, J. Ye, K. Engholm-Keller, P. Højrup, A proteome-scale

study on in vivo protein Nα-acetylation using an optimized method, Proteomics. 11 (2011) 81–93. doi:10.1002/pmic.201000453.
[3] A. Geissenhöner, C. Weise, A.E. Ehrenhofer-Murray, Dependence of ORC silencing function on NatA-mediated Nalpha acetylation in Saccharomyces cerevisiae, Mol Cell Biol. 24 (2004) 10300–10312. doi:10.1128/MCB.24.23.10300-10312.2004.
[4] X. Wang, J.J. Connelly, C.-L. Wang, R. Sternglanz, Importance of the Sir3 N terminus and its acetylation for yeast transcriptional silencing, Genetics. 168 (2004) 547–551. doi:10.1534/genetics.104.028803.
[5] M. Altaf, R.T. Utley, N. Lacoste, S. Tan, S.D. Briggs, J. Côté, Interplay of chromatin modifiers on a short basic patch of histone H4 tail defines the boundary of telomeric heterochromatin, Mol Cell. 28 (2007) 1002–1014. doi:10.1016/j.molcel.2007.12.002.
[6] T. van Welsem, F. Frederiks, K.F. Verzijlbergen, A.W. Faber, Z.W. Nelson, D.A. Egan, et al., Synthetic lethal screens identify gene silencing processes in yeast and implicate the acetylated amino terminus of Sir3 in recognition of the nucleosome core, Mol Cell Biol. 28 (2008) 3861–3872. doi:10.1128/MCB.02050-07.
[7] C.H. Yi, H. Pan, J. Seebacher, I.-H. Jang, S.G. Hyberts, G.J. Heffron, et al., Metabolic Regulation of Protein N-Alpha-Acetylation by Bcl-xL Promotes Cell Survival, Cell. 146 (2011) 607–620. doi:10.1016/j.cell.2011.06.050.
[8] K. Kobayashi, L.W. Lin, J.E. Yeadon, L.B. Klickstein, J.A. Smith, Cloning and sequence analysis of a rat liver cDNA encoding acyl-peptide hydrolase, J Biol Chem. 264 (1989) 8892–8899.
[9] A. Adibekian, B.R. Martin, C. Wang, K.-L. Hsu, D.A. Bachovchin, S. Niessen, et al., Click-generated triazole ureas as ultrapotent in vivo-active serine hydrolase inhibitors, Nat. Chem. Biol. 7 (2011) 469–478. doi:10.1038/nchembio.579.
[10] T. Fujino, K. Ando, M. Beppu, K. Kikugawa, Enzymatic removal of oxidized protein aggregates from erythrocyte membranes, J Biochem. 127 (2000) 1081–1086.
[11] T. Fujino, K. Watanabe, M. Beppu, K. Kikugawa, H. Yasuda, Identification of oxidized protein hydrolase of human erythrocytes as acylpeptide hydrolase, Biochim Biophys Acta. 1478 (2000) 102–112.
[12] H. Gonen, C.E. Smith, N.R. Siegel, C. Kahana, W.C. Merrick, K. Chakraburtty, et al., Protein synthesis elongation factor EF-1 alpha is essential for ubiquitin-dependent degradation of certain N alpha-acetylated proteins and may be substituted for by the bacterial elongation factor EF-Tu, Proc Natl Acad Sci USA. 91 (1994) 7648–7652.
[13] A. Hershko, H. Heller, E. Eytan, G. Kaklij, I.A. Rose, Role of the alpha-amino group of protein in ubiquitin-mediated protein breakdown, Proc Natl Acad Sci USA. 81 (1984) 7021–7025.
[14] G. Palmieri, P. Bergamo, A. Luini, M. Ruvo, M. Gogliettino, E. Langella, et al., Acylpeptide hydrolase inhibition as targeted strategy to induce proteasomal down-regulation, PLoS ONE. 6 (2011) e25888. doi:10.1371/journal.pone.0025888.

[15] W.M. Jones, A. Scaloni, F. Bossa, A.M. Popowicz, O. Schneewind, J.M. Manning, Genetic relationship between acylpeptide hydrolase and acylase, two hydrolytic enzymes with similar binding but different catalytic specificities, Proc Natl Acad Sci USA. 88 (1991) 2194–2198.
[16] N. Iles, S. Rulten, S.F. El-Khamisy, K.W. Caldecott, APLF (C2orf13) is a novel human protein involved in the cellular response to chromosomal DNA strand breaks, Mol Cell Biol. 27 (2007) 3793–3803. doi:10.1128/MCB.02269-06.
[17] S. Kadkhodayan, E.P. Salazar, J.E. Lamerdin, C.A. Weber, Construction of a functional cDNA clone of the hamster ERCC2 DNA repair and transcription gene, Somat Cell Mol Genet. 22 (1996) 453–460.
[18] K. Takayama, E.P. Salazar, A. Lehmann, M. Stefanini, L.H. Thompson, C.A. Weber, Defects in the DNA repair and transcription gene ERCC2 in the cancer-prone disorder xeroderma pigmentosum group D, Cancer Res. 55 (1995) 5656–5663.
[19] T.R. Brummelkamp, R. Bernards, R. Agami, A system for stable expression of short interfering RNAs in mammalian cells, Science. 296 (2002) 550–553. doi:10.1126/science.1068999.
[20] K.W. Caldecott, S. Aoufouchi, P. Johnson, S. Shall, XRCC1 polypeptide interacts with DNA polymerase beta and possibly poly (ADP-ribose) polymerase, and DNA ligase III is a novel molecular “nick-sensor” in vitro, Nucleic Acids Res. 24 (1996) 4387–4394.
[21] P.M. Clements, C. Breslin, E.D. Deeks, P.J. Byrd, L. Ju, P. Bieganowski, et al., The ataxia-oculomotor apraxia 1 gene product has a role distinct from ATM and interacts with the DNA strand break repair proteins XRCC1 and XRCC4, DNA Repair (Amst). 3 (2004) 1493–1502. doi:10.1016/j.dnarep.2004.06.017.
[22] J.I. Loizou, S.F. El-Khamisy, A. Zlatanou, D.J. Moore, D.W. Chan, J. Qin, et al., The protein kinase CK2 facilitates repair of chromosomal DNA single-strand breaks, Cell. 117 (2004) 17–28.
[23] A. Marintchev, A. Robertson, E.K. Dimitriadis, R. Prasad, S.H. Wilson, G.P. Mullen, Domain specific interaction in the XRCC1-DNA polymerase beta complex, Nucleic Acids Res. 28 (2000) 2049–2059.
[24] C.J. Whitehouse, R.M. Taylor, A. Thistlethwaite, H. Zhang, F. Karimi-Busheri, D.D. Lasko, et al., XRCC1 stimulates human polynucleotide kinase activity at damaged DNA termini and accelerates DNA single-strand break repair, Cell. 104 (2001) 107–117.
[25] A. Marintchev, M.A. Mullen, M.W. Maciejewski, B. Pan, M.R. Gryk, G.P. Mullen, Solution structure of the single-strand break repair protein XRCC1 N-terminal
domain, Nat Struct Mol Biol. 6 (1999) 884–893. doi:doi:10.1038/12347.
[26] C. Breslin, K.W. Caldecott, DNA 3'-phosphatase activity is critical for rapid global rates of single-strand break repair following oxidative stress, Mol Cell Biol. 29 (2009) 4653–4662. doi:10.1128/MCB.00677-09.
[27] A. Marintchev, M.R. Gryk, G.P. Mullen, Site-directed mutagenesis

analysis of the structural interaction of the single-strand-break repair protein, X-ray cross-complementing group 1, with DNA polymerase beta, Nucleic Acids Res. 31 (2003) 580–588.
[28] K. Shimizu, Y. Kiuchi, K. Ando, M. Hayakawa, K. Kikugawa, Coordination of oxidized protein hydrolase and the proteasome in the clearance of cytotoxic denatured proteins, Biochem Biophys Res Commun. 324 (2004) 140–146. doi:10.1016/j.bbrc.2004.08.231.
[29] K.W. Caldecott, Single-strand break repair and genetic disease, Nat. Rev. Genet. 9 (2008) 619–631. doi:10.1038/nrg2380.
[30] J.J. Reynolds, A.K. Walker, E.C. Gilmore, C.A. Walsh, K.W. Caldecott, Impact of PNKP mutations associated with microcephaly, seizures and developmental delay on enzyme activity and DNA strand break repair, Nucleic Acids Res. (2012). doi:10.1093/nar/gks318.
[31] A. Scaloni, W.M. Jones, D. Barra, M. Pospischil, S. Sassa, A. Popowicz, et al., Acylpeptide hydrolase: inhibitors and some active site residues of the human enzyme, J Biol Chem. 267 (1992) 3811–3818.
[32] K. Shimizu, T. Fujino, K. Ando, M. Hayakawa, H. Yasuda, K. Kikugawa, Overexpression of oxidized protein hydrolase protects COS-7 cells from oxidative stress-induced inhibition of cell growth and survival, Biochem Biophys Res Commun. 304 (2003) 766–771.
[33] S. Bekker-Jensen, K. Fugger, J.R. Danielsen, I. Gromova, M. Sehested, J. Celis, et al., Human Xip1 (C2orf13) is a novel regulator of cellular responses to DNA strand breaks, J Biol Chem. 282 (2007) 19638–19643. doi:10.1074/jbc.C700060200.
[34] H. Luo, D.W. Chan, T. Yang, M. Rodriguez, B.P.-C. Chen, M. Leng, et al., A new XRCC1-containing complex and its role in cellular survival of methyl methanesulfonate treatment, Mol Cell Biol. 24 (2004) 8356–8365. doi:10.1128/MCB.24.19.8356-8365.2004.
[35] X-ray induced DNA double strand break production and repair in mammalian cells as measured by neutral filter elution, 7 (1979) 793–804. http://eutils.ncbi.nlm.nih.gov/entrez/eutils/elink.fcgi?dbfrom=pubmed&id=92010&retmode=ref&cmd=prlinks.
[36] T. Fujino, T. Tada, M. Beppu, K. Kikugawa, Purification and characterization of a serine protease in erythrocyte cytosol that is adherent to oxidized membranes and preferentially degrades proteins modified by oxidation and glycation, J Biochem. 124 (1998) 1077–1085.
[37] D. Cervantes-Laurean, E.L. Jacobson, M.K. Jacobson, Glycation and glycoxidation of histones by ADP-ribose, J Biol Chem. 271 (1996) 10461–10469.
[38] S. Guedes, R. Vitorino, M.R.M. Domingues, F. Amado, P. Domingues, Glycation and oxidation of histones H2B and H1: in vitro study and characterization by mass spectrometry, Anal Bioanal Chem. 399 (2011) 3529–3539. doi:10.1007/s00216-011-

4679-y.
[39] G.T. Wondrak, D. Cervantes-Laurean, E.L. Jacobson, M.K. Jacobson, Histone carbonylation in vivo and in vitro, Biochem J. 351 Pt 3 (2000) 769–777.
[40] T. Jiang, X. Zhou, K. Taghizadeh, M. Dong, P.C. Dedon, N-formylation of lysine in histone proteins as a secondary modification arising from oxidative DNA damage, Proc Natl Acad Sci USA. 104 (2007) 60–65. doi:10.1073/pnas.0606775103.
[41] O. Ullrich, T. Reinheckel, N. Sitte, R. Hass, T. Grune, K.J. Davies, Poly-ADP ribose polymerase activates nuclear proteasome to degrade oxidatively damaged histones, Proc Natl Acad Sci USA. 96 (1999) 6223–6228.
[42] B. Catalgol, B. Wendt, S. Grimm, N. Breusing, N.K. Ozer, T. Grune, Chromatin repair after oxidative stress: role of PARP-mediated proteasome activation, Free Radic. Biol. Med. 48 (2010) 673–680. doi:10.1016/j.freeradbiomed.2009.12.010.

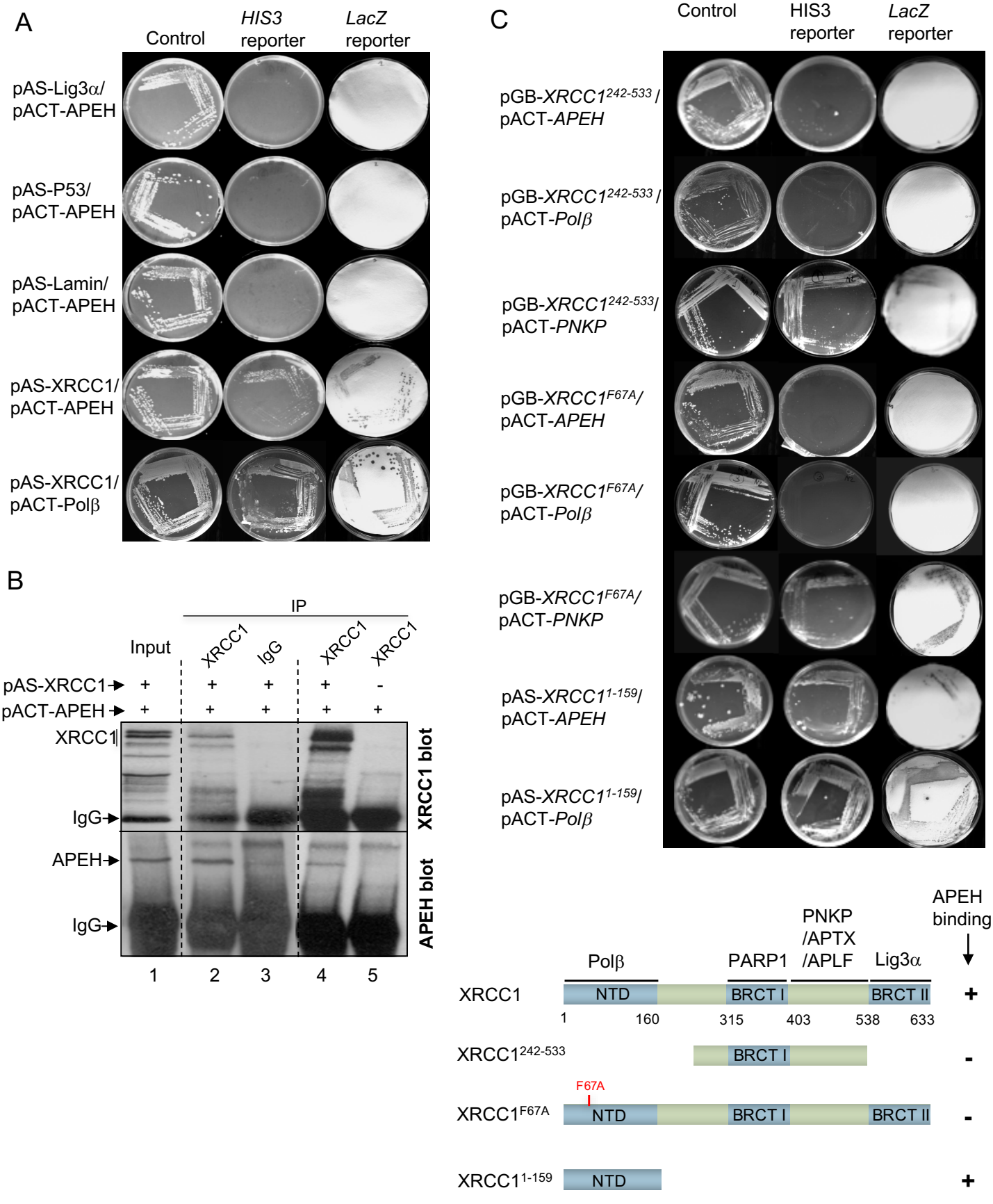
A
Control
HIS3 reporter
LacZ reporter
pAS-Lig3α/ pACT-APEH
pAS-P53/ pACT-APEH
pAS-Lamin/ pACT-APEH
pAS-XRCC1/ pACT-APEH
pAS-XRCC1/ pACT-Polβ
B
IP
Input
XRCC1
IgG
XRCC1
XRCC1
pAS-XRCC1
pACT-APEH
XRCC1
IgG
APEH
IgG
XRCC1 blot
APEH blot
1 2 3 4 5
C
Control
HIS3 reporter
LacZ reporter
pGB-XRCC1242-533 / pACT-APEH
pGB-XRCC1242-533 / pACT-Polβ
pGB-XRCC1242-533/ pACT-PNKP
pGB-XRCC1F67A/ pACT-APEH
pGB-XRCC1F67A/ pACT-Polβ
pGB-XRCC1F67A/ pACT-PNKP
pAS-XRCC11-159/ pACT-APEH
pAS-XRCC11-159/ pACT-Polβ
APEH binding
Polβ
PARP1
PNKP /APTX /APLF
Lig3α
XRCC1
NTD
BRCT I
BRCT II
1
160
315
403
538
633
XRCC1242-533
F67A
XRCC1F67A
XRCC11-159

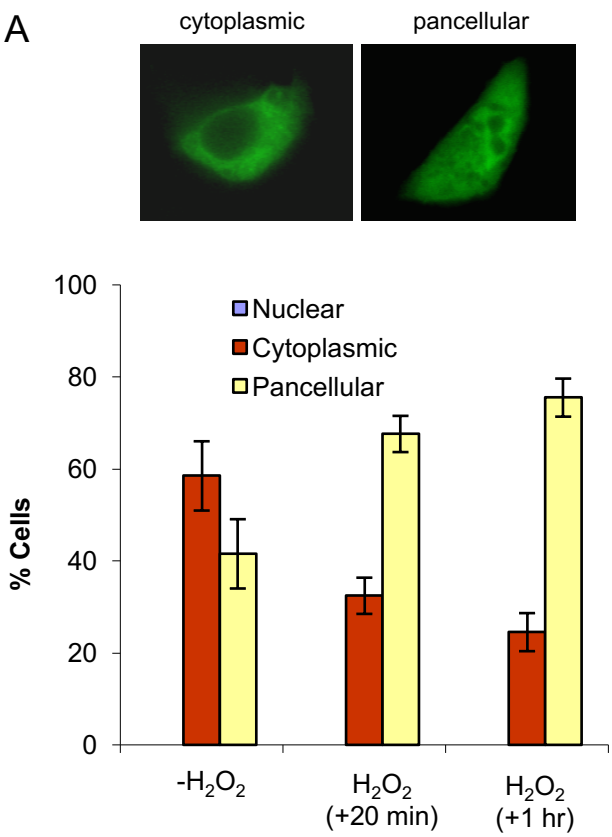
A
cytoplasmic
pancellular
100
80
60
40
20
0
% Cells
Nuclear
Cytoplasmic
Pancellular
-H2O2
H2O2
(+20 min)
H2O2
(+1 hr)

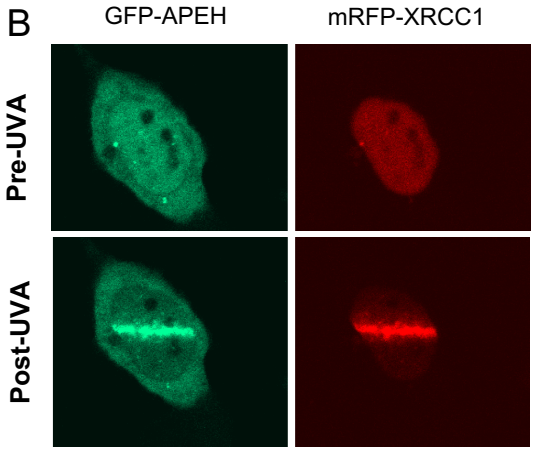
B
GFP-APEH
mRFP-XRCC1
Pre-UVA
Post-UVA

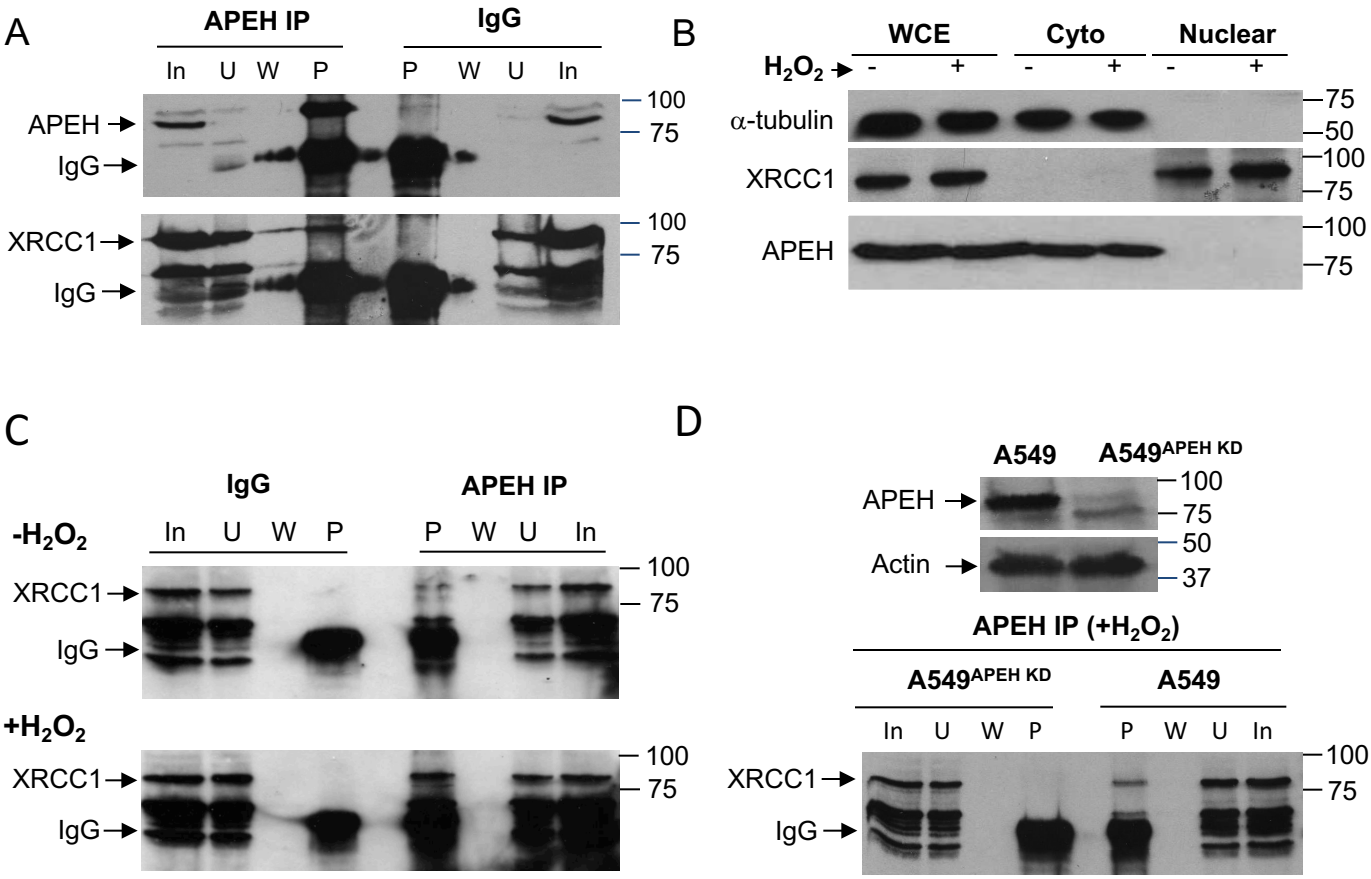
A
APEH IP
IgG
In U W P
P W U In
APEH
IgG
XRCC1
IgG
100
75
100
75
B
WCE
Cyto
Nuclear
H2O2
- + - + - +
α-tubulin
XRCC1
APEH
75
50
100
75
100
75
C
IgG
APEH IP
-H2O2
In U W P
P W U In
XRCC1
IgG
+H2O2
XRCC1
IgG
100
75
100
75
D
A549
A549APEH KD
APEH
Actin
100
75
50
37
APEH IP (+H2O2)
A549APEH KD
A549
In U W P
P W U In
XRCC1
IgG
100
75

A

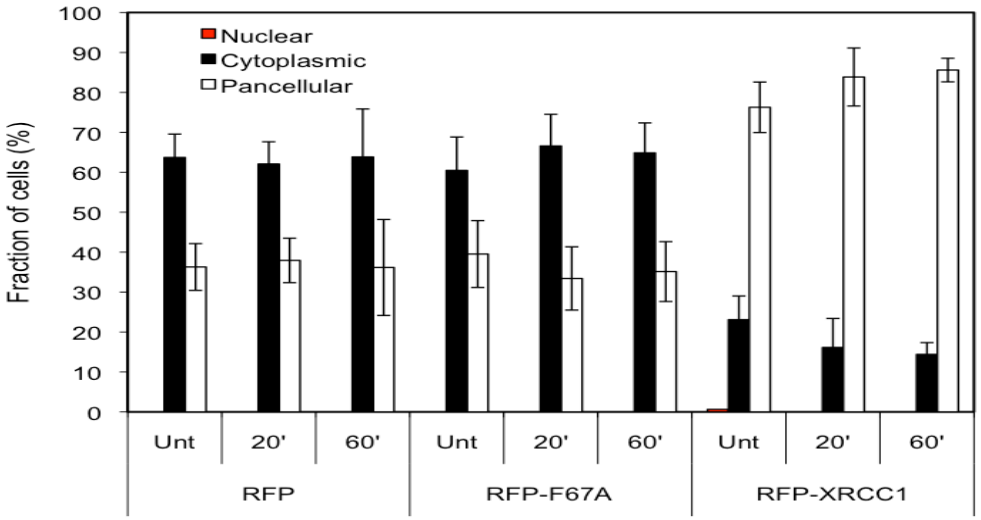
Nuclear
Cytoplasmic
Pancellular
Fraction of cells (%)
100
90
80
70
60
50
40
30
20
10
0
Unt
20'
60'
Unt
20'
60'
Unt
20'
60'
RFP
RFP-F67A
RFP-XRCC1

B

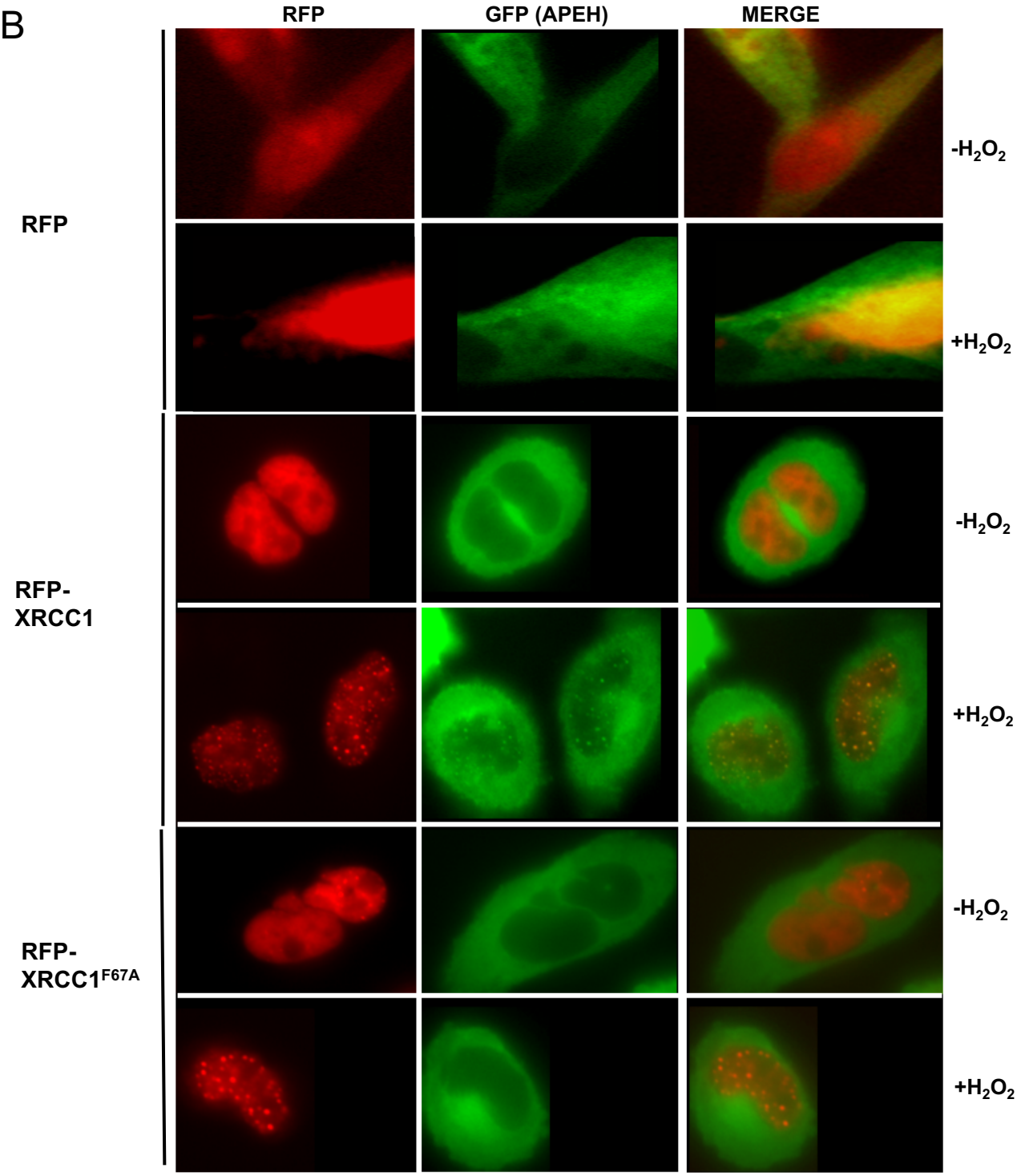
RFP
GFP (APEH)
MERGE
RFP
RFP-XRCC1
RFP-XRCC1F67A
-H2O2
+H2O2
-H2O2
+H2O2
-H2O2
+H2O2

A

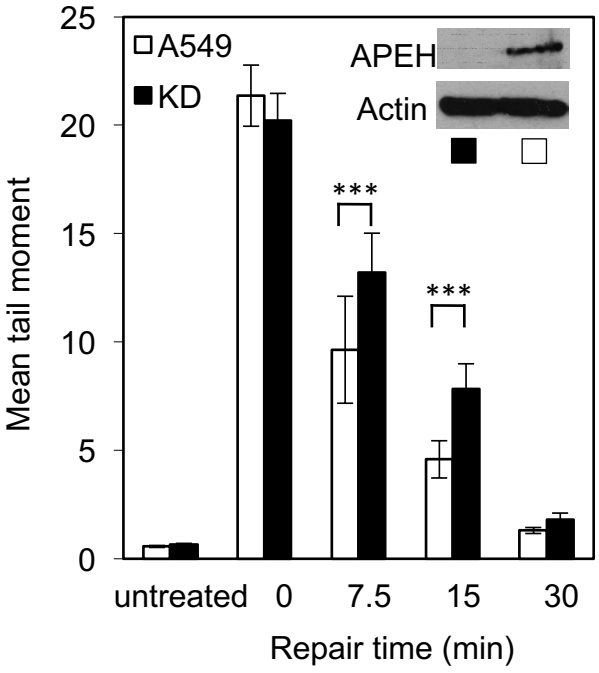
A549
KD
APEH
Actin
***
***
Mean tail moment
25
20
15
10
5
0
untreated
0
7.5
15
30
Repair time (min)

B

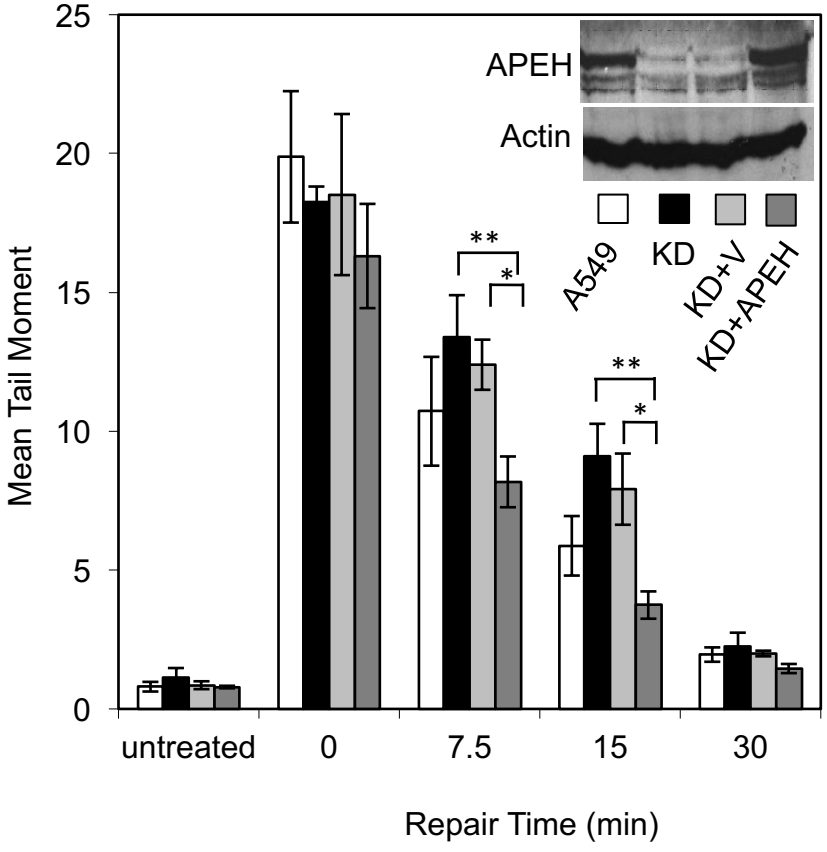
APEH
Actin
A549
KD
KD+V
KD+APEH
**
*
**
*
Mean Tail Moment
25
20
15
10
5
0
untreated
0
7.5
15
30
Repair Time (min)

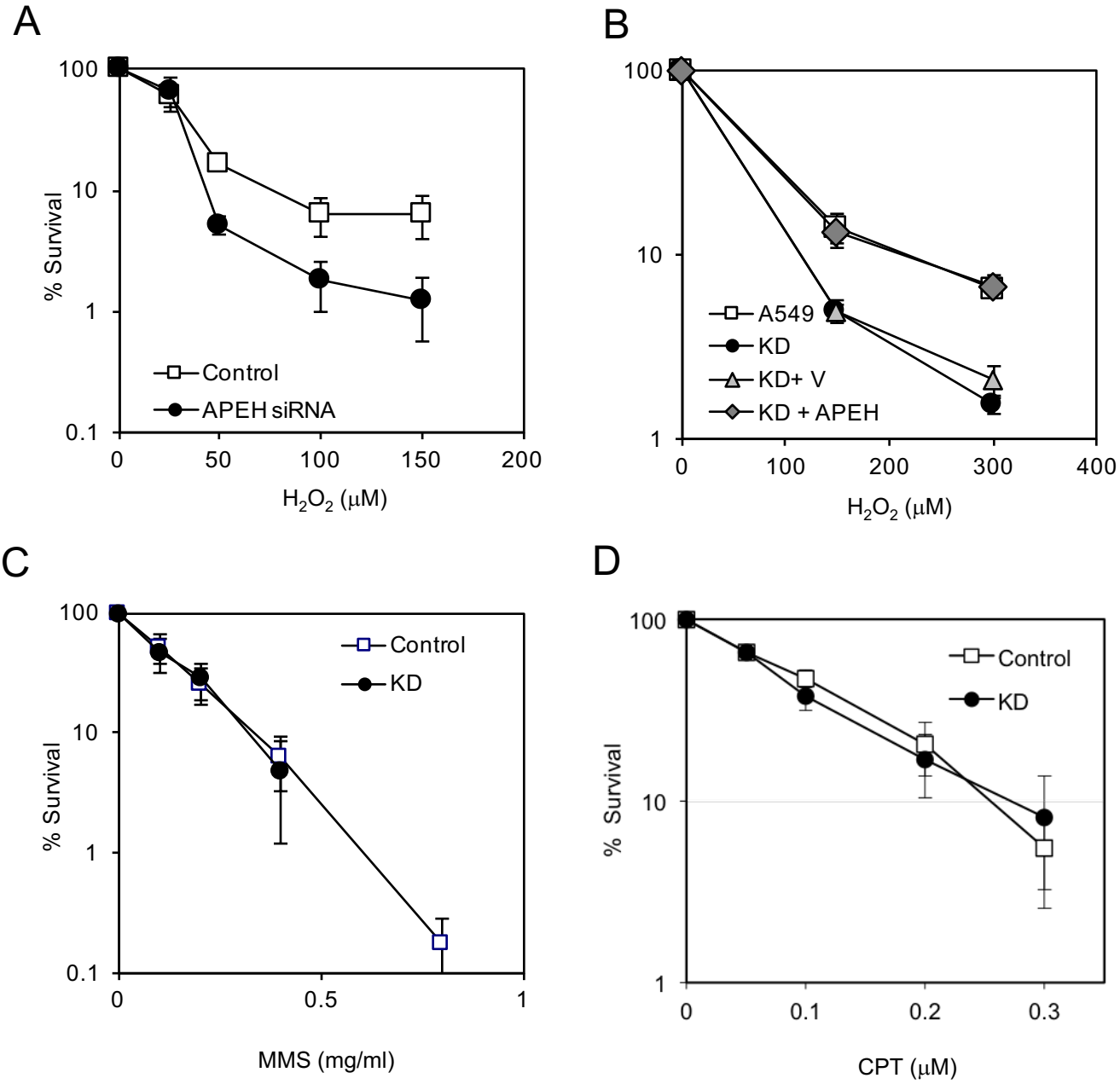
A
100
10
1
0.1
% Survival
Control
APEH siRNA
0
50
100
150
200
H2O2 (μM)
B
100
10
1
A549
KD
KD+ V
KD + APEH
0
100
200
300
400
H2O2 (μM)
C
100
10
1
0.1
% Survival
Control
KD
0
0.5
1
MMS (mg/ml)
D
100
10
1
% Survival
Control
KD
0
0.1
0.2
0.3
CPT (μM)